ResearchSpace@Auckland

Version

This is the Accepted Manuscript version. This version is defined in the NISO recommended practice RP-8-2008 http://www.niso.org/publications/rp/

Suggested Reference

Copyright

Time dependent prestress losses in historic clay brick masonry walls seismically strengthened using unbonded posttensioning

Najif Ismail, S.M. ASCE

Senior Lecturer, School of Architecture Building and Engineering, Otago Polytechnic, Private Bag 1910, Dunedin 9054, New Zealand; najif.ismail@op.ac.nz

Jason M. Ingham, M. ASCE

Associate Professor, Department of Civil & Environmental Engineering, University of Auckland, Private Bag 92019, Auckland 1142, New Zealand; j.ingham@auckland.ac.nz

Abstract

Time dependent prestress losses in historic unreinforced clay brick masonry (URM) walls strengthened using unbonded posttensioning were investigated, with a particular emphasis on masonry shortening resulting due to creep and shrinkage. An experimental program was undertaken that involved continuous monitoring of masonry shortening occurring in prestressed URM wallettes over a period of 180 days. The test wallettes were extracted from a real historic URM building and were subjected to varying magnitudes of prestress, representing axial stresses that would be developed at the wall base when strengthened using unbonded posttensioning. A rheological model is proposed for predicting masonry creep shortening, which can subsequently be used to predict posttensioning losses. It was established that a prestress loss of up to 16.4% for normal threaded steel bars and up to 5.4% for sheathed greased seven wire strands can be expected in posttensioned historic URM walls when the tendons are posttensioned to a stress of $0.5f_{pu}$.

Keywords

Time dependent losses; masonry; seismic strengthening; masonry creep; masonry shrinkage; posttensioning.

1

Introduction

Current masonry codes provide guidelines for assessing posttensioning (PT) losses, with these losses typically attributed to shrinkage, creep, tendon relaxation, elastic shortening, anchorage seating, tendon undulation, friction and thermal effects (AS 2001; BS 2000; CEN 2005; CSA 2004; MSJC 2008; NZS 2004; PCI 1975). Of these factors, steel relaxation, shrinkage and creep are the most important factors that will influence the design and longevity of an adequate retrofit. However, for historic clay brick masonry walls shrinkage losses or masonry expansion are unlikely to be large because of the significant age of the masonry materials. For analysis and design of prestressed masonry an effective prestress f_{se} is calculated using Equation 1, which is defined as the PT stress after all losses have occurred. In Equation 1, the total PT stress loss Δf_{pl} is the sum of PT losses due to tendon relaxation, masonry shrinkage and masonry creep (refer Equation 2).

$$f_{se} = f_{psi} - \Delta f_{pl} \tag{1}$$

$$\Delta f_{pl} = \Delta f_{sh} + \Delta f_{cr} + \Delta f_{pr} \tag{2}$$

where f_{psi} = initially applied PT stress, Δf_{pr} = PT stress loss due to steel relaxation, Δf_{sh} = PT stress loss due to masonry shrinkage, and Δf_{cr} = PT stress loss due to masonry creep shortening. More masonry shortening is expected in historic URM walls than in newly constructed URM walls due to the presence of relatively larger amount of highly deformable bed joint mortar. However, as historic masonry walls have already been subjected to sustained overburden weights for a considerable span of time, which is likely to have resulted in expulsion of water and air voids, suggesting the masonry shortening to be less in historic masonry than in new URM construction. These unique characteristics of historic URM walls suggest that prestress losses due to masonry shrinkage and creep shortening can be expected to be significantly different from that observed in new URM construction, motivating the

48   initiation of an experimental investigation of masonry shrinkage and creep shortening in real

49   historic URM wallettes. Some experimental studies have already investigated the PT losses in

50   historic clay brick masonry but because of the large variation observed between the results of

51   these studies and the typical codified PT loss parameters, there still exists considerable

52   uncertainty. Therefore, an experimental program investigating the time dependent shortening

53   in historical URM walls was undertaken.

54   *PT losses due to tendon relaxation*

55   Tendon relaxation losses, Δf_{pr}, are influenced by the tendon type (constituent steel properties)

56   and the end anchorage details, which are normally quantified as a percentage of the initially

57   applied tendon stress, f_{psi}. The relaxation loss parameter, k_r, is normally provided by the PT

58   tendon manufacturer, which is experimentally determined over a period of 1000 hours.

59   Literature suggests the ultimate relaxation losses to be 3 times the value suggested for 1000

60   hours (CEN 2005). The Prestressed Concrete Institute recommended Equation 3 (PCI 1975)

61   to establish relaxation loss at any given time after prestressing, which was later adapted by

62   Laursen (2002) to determine the ultimate relaxation loss for a PT strand and is reproduced

63   herein as Equation 4.

$$\Delta f_{pr} = f_{psi}\left[\frac{Log_{10}^{t}}{45}\left(\frac{f_{psi}}{f_{py}} - 0.55\right)\right] \text{ for } \frac{f_{psi}}{f_{py}} \geq 0.55 \tag{3}$$

$$\Delta f_{pr} = k_r f_{psi} \times 3.7\left(\frac{f_{psi}}{f_{py}} - 0.55\right) \tag{4}$$

64   where t = time since the application of PT stress and f_{py} = nominal specified tendon tensile

65   yield strength.

66   ***PT losses due to masonry shrinkage and creep***

67   Masonry undergoes deformation when subjected to sustained loading over long periods of

68   time, which eventually causes axial shortening in prestressed masonry. The axial shortening

69   due to sustained axial loading is termed as creep. Typically, masonry creep is quantified by a

70   creep parameter, k_c (also known as specific creep), which is defined as creep strain per MPa

71   of initially applied sustained prestress and depends upon the constituent masonry materials.

72   Another widely accepted parameter for quantifying masonry creep shortening is the masonry

73   creep ratio (also referred to as ultimate creep compliance), C_c, which is the ratio of the long

74   term masonry shortening to the initial elastic masonry shortening.

75   It should also be noted that shrinkage of masonry occurs due to drying process of the mortar,

76   which is unlikely to happen in historic URM buildings considered for a PT seismic retrofit

77   because of the significant age of the masonry. Equations 5 and 6 show the relations to

78   evaluate the PT losses due to masonry shrinkage and creep respectively, where it is

79   anticipated that the masonry stress due to applied prestress, overburden weights and self

80   weight of the wall is less than 0.7 times the masonry compressive strength.

$$\Delta f_{sh} = k_{sh} \frac{P_{psi}}{b_w l_w} E_{ps} \tag{5}$$

$$\Delta f_{cr} = \frac{C_c}{E_m} \frac{P_{psi}}{b_w l_w} E_{ps} \tag{6}$$

81   In addition to these long term deformations, an immediate elastic shortening occurs in

82   masonry when prestress is applied, which can be calculated using the masonry elastic

83   modulus. As the monitoring of masonry shortening over the entire design life of the structure

84   (typically 50 years) is not practical, the creep strain monitored over a short period of time

4

85 (only after the creep strain curve had levelled out) can be extrapolated using a rheological

86 model. Figure 1 shows an illustration of the masonry shortening occurring in prestressed

87 masonry walls, where t_o is the time when PT is applied and the dotted lines show the losses

88 that can occur in new URM construction but that are less likely to occur in historic URM

89 walls. Note that time dependent masonry shortening also varies due to masonry material

90 degradation and that masonry shortening in realistic URM walls results in variable prestress

91 instead of remaining constant (Anand and Rahman 1991), suggesting the use of an

92 incremental or superposition procedure to be more appropriate to estimate masonry

93 shortening than the additive approach adopted herein. However, such incremental analysis is

94 laborious and its routine utilisation in design practice is questionable.

95 ***Prediction of masonry creep shortening***

96 Based on the results of in-situ and laboratory based creep testing Leczner (1986a) suggested

97 that the creep ratio for prestressed URM walls can be predicted using Equation 7, where f_b is

98 the brick compressive strength. However, Equation 7 was observed to over predict the creep

99 strains when compared to the results of the experimental study presented herein.

$$C_c = 4.46 - 0.33\sqrt{f_b} \qquad (7)$$

100 Rheological models represent the time-dependant visco-elastic behaviour of masonry using

101 different arrangements of springs and dashpots and are typically used for predicting time

102 dependent masonry creep shortening. Of these rheological models the Maxwell model,

103 Kelvin model and Burgers Model are most commonly used (England and Jordaan 1975;

104 Jordaan et al. 1977; Shrive et al. 1997), with the former two consisting of a spring and a

105 dashpot (refer to Figure 2a and 2b) and the third consisting of two springs and two dashpots

106 (refer Figure 2c) that is believed to allow better representation of the masonry creep

107 phenomenon than do the former two. Equations 8 to 10 represent the Maxwell model, Kelvin

108   model and Burgers model respectively, where $\varepsilon_c(t)$ is the sum of elastic shortening strain and

109   the continued creep shortening, λ is the parameter related to delayed strain response of

110   masonry, E_m is the masonry modulus of elasticity, f_{mi} is the magnitude of initially applied

111   prestress, and t is the time in days after prestressing.

$$\varepsilon_c(t) = \frac{f_{mi}}{E_m} + \frac{f_{mi}}{\lambda}t \tag{8}$$

$$\varepsilon_c(t) = \frac{f_{mi}}{E_m}(1 - e^{-\frac{E_m}{\lambda}t}) \tag{9}$$

$$\varepsilon_c(t) = \frac{f_{mi}}{E_m} + \frac{f_{mi}}{\lambda}t + \frac{f_{mi}}{E_m}\left(1 - e^{-\frac{E_m}{\lambda}t}\right) \tag{10}$$

112   Based on the results of in-situ creep testing Hughes and Harvey (1995) established Equation

113   11 to determine the parameter for delayed strain response of masonry, where E_m is the

114   masonry modulus of elasticity in MPa.

$$\lambda = \frac{E_m}{0.112 - 3.35E_m \times 10^{-6}} \tag{11}$$

115   Shrive et al. (1997) substituted for the value of λ from Equation 10 into a modified Burgers

116   model and established Equation 12 for calculation of the creep ratio after t days from the

117   application of prestress, $C_c(t)$.

$$C_c(t) = (0.112 - 3.35E_m \times 10^{-6})t^{0.3} + (1 - e^{-(0.112-3.35E_m\times10^{-6})t}) \tag{12}$$

118   where E_m is the masonry modulus of elasticity in MPa, and t is the time in days from the

119   application of prestress. The predicted creep ratio is then multiplied by an aging coefficient χ

120   (refer Equation 13) to account for the significant age of the masonry that has already been

121   subjected to sustained overburden loading for numerous years. The aging coefficient has

122   previously been used in prestressed concrete design (Ghali and Favre 1986), and was

123   determined herein empirically to match the experimental curves.

$$C_c(t) = \chi\left[(0.112 - 3.35E_m \times 10^{-6})t^{0.3} + (1 - e^{-(0.112-3.35E_m \times 10^{-6})t})\right] \qquad (13)$$

124 ***Precedent experimental programs investigating masonry creep***

125 Several research studies have investigated the nature and magnitude of PT losses that occur in

126 post-tensioned masonry, including the experimental programs discussed below. Schubert &

127 Wesche (1984) proposed creep and shrinkage parameters for concrete and clay brick masonry

128 which are reported in Table 1. Lenczner (1986b) studied the creep strain of a historic URM

129 tower block located in the United Kingdom over a period of eight years and found the total

130 masonry shortening to be roughly twice the magnitude of initial elastic shortening. Studies

131 have also reported creep strain causing failure of historic URM buildings (Binda et al. 1992),

132 emphasising the importance of masonry creep when considering the longevity of PT

133 strengthening of historic URM buildings.

134 Curtin et al. (1982) estimated PT loss by monitoring masonry shortening strains in

135 prestressed URM assemblages and suggested that a PT loss of up to 20% can be expected in

136 newly constructed clay brick masonry walls. Hughes and Harvey (1995) observed the creep

137 strain of a nine storey URM building over 6000 days (with individual test results spanning

138 over 400 days) and observed the creep coefficient, C_c, to range from 0.3 to 3.0. Anand and

139 Bhatia (1996) investigated the creep strain in URM walls, by monitoring the creep strain in

140 several prestressed URM wall specimens over a period of 300 days and by performing micro-

141 level finite element analysis of URM piers over an extended period of time. The study

142 suggested that the long term creep strain can be conservatively estimated by using a masonry

143 creep ratio of 1.5.

144 Shrive et al. (1997) investigated the creep shortening occurring in clay brick masonry walls

145 by monitoring creep strains of a total of 188 five brick high clay brick masonry prisms, which

146   were subjected to varying magnitudes of prestress. The test prisms were constructed using

147   different mortar compositions and were tested in moist and dry conditions. The test prisms

148   were prestressed using symmetrically located high strength threaded steel bars. Series 1 of the

149   testing program had strength and stiffness characteristics similar to prevalent heritage URM

150   materials and therefore the results of only series 1 are used herein. Experimentally

151   determined values of creep parameters for clay brick masonry reported in the aforementioned

152   research studies, together with the codified values of these masonry creep parameters, are

153   presented in Table 1.

Masonry shrinkage and creep testing

155   A total of six URM wallettes extracted from a historic URM building known to be originally

156   constructed in 1881 were subjected to varying magnitudes of prestress and the resulting

157   masonry shortening was monitored over a period of 180 days. All test wallettes were capped

158   using dental plaster to uniformly distribute the prestress over the entire contact surface, which

159   were subsequently prestressed to represent the axial stresses developed at the base of a typical

160   posttensioned historic URM wall. The geometric dimensions of test wallettes and the

161   magnitude of applied prestress are given in Table 2. Test wallettes were given the notation

162   WAB-N or WPT-N, where W refers to wallettes, AB refers to as-built control wallette, PT

163   refers to prestressed wallettes, and N denotes the test number.

Material properties

165   Testing was conducted on URM wallettes extracted from a heritage URM building (hereafter

166   referred to as the Old Supreme Court) situated at Wellington, New Zealand. The old Supreme

167   Court was originally constructed in 1881 and served as the Supreme Court for 100 years up to

168   1980, when it was vacated and fell into decline. The building possesses considerable heritage

169   value and is registered as a category I historic building (building having special historical

170 significance) on the New Zealand Historic Places Trust Register. Given the historic value

171 associated with the Old Supreme Court, the building was carefully strengthened in 2008

172 using lead bearing base isolators and by plastering the URM walls inside and out. Figure 3

173 shows a photograph of the Old Supreme Court when the building was being strengthened in

174 2008. A URM section was extracted from the building when it was being strengthened, which

175 was transported back to the civil test hall at the University of Auckland for material testing.

176 The extracted masonry section was then cut into small URM wallettes using a wet concrete

177 cutting saw (refer Figure 4).

178 The load bearing URM walls of the building consisted of a low strength hydraulic mortar and

179 burnt clay bricks, being on average 70 mm × 110 mm × 210 mm in size. Peripheral walls had

180 a strong cement based plaster on the exterior and the interior faces. In early nineteenth

181 century, as a part of one restoration effort, a bituminous coating was applied on the exterior

182 face of the peripheral walls to avoid rain water ingress that in reality created a barrier for

183 water vapors and contributed towards masonry deterioration. The masonry followed a

184 common English bond pattern, with a header course located after every one stretcher course,

185 interconnecting the multiple leafs together.

186 Masonry material properties were determined and reported by Lumantarna (2012), which are

187 reproduced herein for completeness. Masonry flexural bond strength was determined in

188 accordance with ASTM C1072-10 (2010). The brick flexural strength was determined in

189 accordance with AS/NZS 4456-03 (2003) and mortar compressive strength was determined

190 in accordance with ASTM C109-11 (2011). The compressive strength of bricks and masonry

191 were determined in accordance with ASTM C67-11 (2011) and ASTM C1314-11 (2011)

192 respectively. The results of masonry material testing are reported in Table 3 as mean values

193 and corresponding coefficients of variation (COV).

194   *Testing details*

195   Figure 5 shows the test setup used for shrinkage and creep testing. Test wallettes were

196   sandwiched between a steel I-beam and a 50 mm steel bearing plate. Uniform axial stress

197   (prestress) was applied to test wallettes using two externally located 20 mm threaded steel

198   bars, with a heavy coil spring placed at the bottom of each PT bar to roughly maintain the

199   magnitude of applied prestress and to ensure a uniform stress distribution. An assembly

200   consisting of a 200 kN load cell and a 200 kN hydraulic jack was used for the application of

201   pre-selected magnitudes of prestress. Typical hexagonal nut end anchorage assemblies were

202   used for locking off the posttensioning.

203   The elastic masonry shortening was measured during the PT application process, over a

204   gauge length of 100 mm at four different locations on the masonry assemblage, which were

205   marked prior to the application of prestress by mounting eight Demec points directly onto the

206   masonry surface in the uniform stress region. For measuring the continuing masonry

207   shortening strains, a demountable mechanical displacement gauge having a precision of

208   0.002 mm was used (see Figure 6). The displacement gauge was checked throughout the data

209   collection period using an INVAR steel bar, which was known to have a very low coefficient

210   of thermal expansion. Masonry shortening measurements were made over 180 days, with

211   these measurements made twice a day over the first 20 days and subsequently once a week

212   when the masonry creep continued to occur at a relatively slower rate. The masonry

213   shortening curves for all wallettes were observed to stabilize by the time measurement was

214   discontinued.

215   *Testing results*

216   A summary of test results is presented in Table 4. Estimates about the initial elastic masonry

217   shortening were made using a masonry modulus of elasticity of $300f'_m$ (NZSEE 2011), where

218 f'$_m$ is the masonry compressive strength. The predicted elastic masonry shortening values

219 were found to fit well with the experimentally measured values (refer to Table 4). The

220 maximum experimentally measured specific creep values were calculated by dividing the

221 measured masonry creep strain by the magnitude of initially applied prestress and

222 subsequently the corresponding masonry creep ratio values were calculated by dividing the

223 ultimate specific creep by the initial elastic strain per unit applied prestress. It should be noted

224 that these two masonry creep parameters can also be correlated as $C_c = k_c \times E_m$, where E_m is

225 the masonry elastic modulus. A maximum shortening strain of 90 $\mu\varepsilon$ was also observed in the

226 unstressed wallette, which was attributed to the drying of heavily water saturated wallettes

227 (due to the wet cutting process). In precedent experimental programs, it was established that

228 most of the masonry creep occurs within the first year after prestressing (Anand and Bhatia

229 1996; Anand and Rahman 1991; Hughes and Harvey 1995; Lenczner 1986a; Lenczner

230 1986b; Shrive et al. 1997). Therefore, the specific creep and creep ratio values were then

231 extrapolated using the modified Burgers model (refer Equation 13) to conservatively predict

232 the masonry specific creep after 2 years (refer Figure 8d) from the application of prestress.

233 *Ambient air temperature and relative humidity*

234 Figure 7a and 7b show the variation of the ambient air temperature and relative humidity

235 during the testing. Strains measured in unstressed wallette were used to investigate the strain

236 attributed to environmental changes and total experimentally determined shortening strain

237 attributable to masonry creep was calculated as the difference between the total measured

238 shortening strain in prestressed wallettes and that from the unstressed wallette. It should be

239 noted that the ambient environmental conditions during the testing (inside the civil test hall)

240 were considered to result in strains exceeding those expected for walls in a realistic

241 environment, which is characterised by a lower average temperature and relatively higher

242 humidity.

243 *Time dependent masonry creep shortening*

244 The total masonry strain at time t was plotted in Figure 8a against the time since the

245 application of prestress, where the total masonry strain included the initial elastic shortening

246 strain, the continuing masonry creep strain, and the strain attributed to ambient environmental

247 changes. The total masonry strain $\varepsilon(t)$ can be mathematically represented using Equation 14.

$$\varepsilon(t) = \frac{f_{mi}}{E_m} + f_{mi}k_c(t) + \varepsilon_o \tag{14}$$

248 where E_m is the masonry modulus of elasticity, f_{mi} is the applied prestress; $k_c(t)$ is the specific

249 creep at time t, and ε_o is the strain attributed to ambient environmental changes and drying

250 creep. Similarly, time dependent masonry creep shortening strain and masonry specific creep

251 values were calculated and then plotted in Figure 8b and 8c. It was observed during the

252 testing that the majority of creep shortening occurred within the first 60 days after the

253 application of prestress and subsequently the creep curves started to stabilise and masonry

254 shortening continued to occur at a slower rate. The observed masonry creep behaviour is

255 consistent with that observed in other previously performed masonry creep investigations.

256 Additionally, the masonry specific creep was also observed to be directly related to the

257 magnitude of initially applied prestress.

258 *Prestress losses*

259 Figure 9a shows the estimated prestress loss based on the experimentally determined specific

260 creep values and Figure 9b shows the estimated prestress loss based on the extrapolated

261 specific creep values. The magnitude of prestressing loss due to masonry shortening was

262 estimated by considering the masonry material properties presented in Table 1 and the

263 physical characteristics of three typical PT tendons, being threaded steel bars (f_{pu} = 680 MPa

264 and E_{ps} = 200 GPa), high strength threaded steel bars (f_{pu} = 1080 MPa and E_{ps} = 190 GPa),

265 and greased sheathed seven wire strands (f_{pu} = 1750 MPa and E_{ps} = 170 GPa). It is noted that

266 the axial load ratio in real walls is calculated using total prestress due to both the overburden

267 weight and the applied posttensioning, with the former normally being a small fraction of the

268 latter and thus can be ignored to simplify the prestress loss calculations. It can be seen that a

269 PT loss of up to 16.4% can be expected for a normal threaded steel bars (f_{pu} = 680 MPa),

270 whereas high strength steel bars (f_{pu} = 1080 MPa) and a monostrand (f_{pu} = 1750 MPa) are

271 expected to result in relatively smaller prestress losses of up to 9.8% and 5.4% respectively

272 when posttensioned to a tendon stress of $0.5f_{pu}$, where f_{pu} is the ultimate strength of the PT

273 tendon.

Recommended values of PT loss parameters

275 Table 5 presents the recommended values for parameters k_{sh}, C_c, and k_r for a PT seismic

276 retrofit design of historic URM walls. The shrinkage and creep prestress loss parameters for

277 concrete masonry walls were established on the basis of experimental investigations

278 performed by Laursen (2002) and Wight (2006). The relaxation prestress loss parameter (k_r)

279 for typical PT bar and PT strand was established using technical literature provided by the

280 manufacturers. However, it is noted that for different prestressing systems it may vary and be

281 established by interrogating associated technical literature. The shrinkage and creep prestress

282 loss parameters for URM walls were established based on the results from the creep and

283 shrinkage testing reported herein.

Summary and Conclusions

285 Theoretical considerations for the prediction of PT losses and an overview of precedent

286 experimental programs investigating time dependent masonry shortening are first presented,

287 with a particular emphasis given to prestress losses occurring in clay brick masonry walls.

288 Existing rheological models for predicting creep shortening in newly constructed clay brick

masonry walls were discussed and an adapted rheological model with an appropriate aging coefficient was proposed to predict creep shortening occurring in prestressed historic URM walls. An experimental program was undertaken to investigate time dependent masonry shortening, involving the measurement of masonry strains in six (6) prestressed URM wallettes over a period of 180 days. The test wallettes used in the experimental program were extracted from a real historic URM building, which was originally constructed in 1881 and possesses a special historical significance. From experimental results masonry creep coefficients were investigated and were subsequently used to predict time dependent PT losses. The key findings of the experimental program are:

- Large variations between the codified and experimentally determined masonry creep parameters were observed, necessitating further experimental investigations.

- Initial masonry shortening matched the theoretically determined masonry elastic shortening.

- The majority of masonry shortening occurred during the first 60 days from the application of prestress and subsequently the masonry shortening continued to occur at a relatively slower rate until the measurement was discontinued.

- After 180 days from prestressing, the experimentally determined specific creep values ranged from 181 $\mu\varepsilon$/MPa to 234 $\mu\varepsilon$/MPa.

- The specific creep values after 2 years from the application of prestress were estimated using a proposed rheological model that resulted in specific creep values ranging from 209 $\mu\varepsilon$/MPa (analogous to a creep ratio of 0.41) to 278 $\mu\varepsilon$/MPa (analogous to a creep ratio of 0.55).

311 • A prestress loss of 16.4% was estimated to occur when a threaded steel bar (having an

312 ultimate tensile strength of 680 MPa) is posttensioned to a stress of $0.5f_{pu}$, whereas a

313 relatively smaller prestress loss of 5.4% was estimated when a sheathed, greased

314 seven wire strand (having an ultimate tensile strength of 1750 MPa) is posttensioned

315 to a stress of $0.5f_{pu}$, where f_{pu} is the ultimate tensile strength of the tendon.

Acknowledgments

References

323 Anand, S. C., and Bhatia, N. (1996). "Prestress loss due to creep in post-tensioned clay

324 masonry." 1996 CCMS of the ASCE Symposium in Conjunction with Structures

325 Congress XIV, Chicago, USA, 49-60.

326 Anand, S. C., and Rahman, M. A. (1991). "Numerical modelling of creep in composite

327 masonry walls." *Journal of Structural Engineering,*, 117(7), 2149-2165.

328 AS. (2001). *AS 3700-01: Masonry structures*, Standards Australia International, Sydney,

329 NSW, Australia.

330 AS/NZS. (2003). *AS/NZS 4456-03: Masonry Units, Segmental Pavers and Flags - Methods

331 of Test*, Standards Australia, Sydney, Australia.

332   ASTM. (2011). *ASTM C67-11: Standard test methods for sampling and testing brick and structural clay tile*, American Society for Testing and Materials International, West Conshohoken, USA.

335   ASTM. (2011). *ASTM C109-11: Standard test method for compressive strength of hydraulic cement mortars,* American Society for Testing and Materials International, West Conshohoken, USA.

338   ASTM. (2010). *ASTM C1072-10: Standard test method for measurement of masonry flexural bond strength*, American Society for Testing and Materials International, West Conshohoken, USA.

341   ASTM. (2011). *ASTM C1314-11: Standard test method for compressive strength of masonry prisms*, American Society for Testing and Materials International, West Conshohoken, USA.

344   Binda, L., Gatti, G., Mangano, G., Poggi, C., and Sacchi-Landriani, G. (1992). "The collapse of civic tower of Pavia." *Masonry International*, 6(1), 11-20.

346   BS. (2000). *BS 5628:2000-2: British standard code of practice for use of masonry. Part 2: Structural use of reinforced and prestressed masonry*, British Standards Institutation, London, UK.

349   CEN. (2005). *EN 1996-05 - Eurocode 6: Design of masonry structures*, Comite Europeen de Normalisation (European Committee for Standardization), Brussels, Belgium.

351   CSA. (2004). *CSA S304.1-04: Design of masonry structures*, Canadian Standards Association, Mississauga, Ontario, Canada.

353   Curtin, W. G., Shaw, G., Beck, J. K., and Bray, W. (1982). *Structural masonry designer's*

354   *manual*, Blackwell Science Ltd, Oxford.

355   England, G. L., and Jordaan, I. J. (1975). "Time dependant and steady state stress in concrete

356   structures with steel reinforcement at normal and raised temperature." Magazine of

357   Concrete Research, 27(92), 131-142.

358   Ghali, A., and Favre, R. (1986). *Concrete structures: stress and deformations*, Chapman &

359   Hall Ltd., London, United Kingdom.

360   Hughes, T. G., and Harvey, R. J. (1995). "Creep measured in a brick masonry tower block "

361   *Masonry International*, 9(1), 50-56.

362   Jordaan, I. J., England, G. L., and Khalifa, M. A. (1977). "Creep of concrete, a consistent

363   engineering approach." ASCE Journal of the Structural Division, 103(3), 475-491.

364   Laursen, P. T. (2002). "Seismic analysis and design of post-tensioned concrete masonry

365   walls," PhD Thesis, University of Auckland, Auckland.

366   Lenczner, D. (1986a). "Creep and prestress losses in brick masonry." *The Structural*

367   *Engineer*, 64B(3), 57-62.

368   Lenczner, D. (1986b). "In-situ measurements of creep movement in a brick masonry tower

369   block." *Masonry International*, 8(1), 17-20.

370   Lumantarna, R. (2012). "Characterisation of materials in URM buildings in New Zealand,"

371   PhD Thesis, University of Auckland, Auckland, New Zealand.

372   MSJC. (2008). *ACI 530-08/ASCE 5-08/TMS 402-08:Building code requirements for masonry*

373   *structures*, The Masonry Society, Boulder, CO, USA.

374   National Library of New Zealand (2012). "Supreme Court Building, Wellington, New

375   Zealand, [ca 1881]." Photographs of Wellington and district, Reference Number PA-

376   Group-00190, <http://mp.natlib.govt.nz/detail/?id=106914&l=mi>. (19 April 2012,

377   2012).

378   NZSEE. (2011). Assessment and improvement of unreinforced masonry buildings for

379   earthquake resistance, New Zealand Society for Earthquake Engineering, Wellington.

380   PCI. (1975). "Recommendations for estimating prestress losses." *Journal of the Prestressed*

381   *Concrete Institute*, 20(4), 43-75.

382   Schubert, P., and Wesche, K. (1984). *Verformung and Rissesicherheit von Mauerwerk*

383   *(Deformations and cracking behaviour of masonry)*, MauerwerkKalender Ernst &

384   Sohn, Berlin, Germany.

385   Shrive, N. G., Sayed-Ahmed, E. Y., and Tilleman, D. (1997). "Creep analysis of clay

386   masonry assemblages." *Canadian Journal of Civil Engineering*, 24(3), 367-379

387   Wight, G. D. (2006). "Seismic performance of a post-tensioned concrete masonry wall

388   system " PhD Thesis, University of Auckland, Auckland.

389 **Tables**

390 **Table 1.** Masonry shrinkage and creep parameters

Reference	Clay Brick Masonry*			New Concrete Masonry		
	C_c Ratio	k_c με	k_{sh} με	C_c Ratio	k_c με	k_{sh} με
BS 5628 (2000)	1.5	759[#]	0	3.0	210[##]	500
TMS 402 (2008)	0.02[#]	10	0	0.5[##]	36	100
AS 3700 (2001)	0.5-0.6	253-304[#]	0	2.5	170[##]	700
S 304.1 (2004)	1.0-3.0	506-1517[#]	0	3.0-4.0	210-280[##]	100-200
EC 06 (2005)	0.7	354[#]	0	1.5	105[##]	150
Laursen (2002)	-	-	-	1.5-3.4	105-282	373-388
Wight (2006)	-	-	-	1.7-3.4	115-282	435-738
Schubert & Wesche (1984)	0.5-1.7	253-860[#]	0	-	-	-
Lenczner (1986b)	2.0**	1011[#]	0	-	-	-
Shrive et al. (1997)	0.5-1.7	253-860[#]	0	-	-	-
Anand & Bhatia (1996)	1.5	759[#]	0	-	-	-

Where: C_c = masonry creep ratio; k_c = masonry specific creep; and k_{sh} = masonry shrinkage parameter.
*old masonry with weak hydraulic mortar and saturated bricks, **found experimentally over a period of 8 years in a historic URM building located in UK, [#]analogous value calculated using $E_m = 300f'_m$ and $f'_m = 6.59$ MPa, [##]analogous value calculated using $E_m = 800f'_m$ and $f'_m = 18$ MPa (Wight 2006)

391

392 **Table 2.** Masonry shrinkage and creep testing details

Wallette	B (mm)	H (mm)	T (mm)	f'_m MPa	A_g mm^2	P_{psi} (kN)	f_{mi} (MPa)	f_{mi}/f'_m (Ratio)
WPT – 01	236	232	126	6.59	29232	30.11	1.03	0.16
WPT – 02	239	200	140	6.59	28000	23.24	0.83	0.13
WPT – 03	230	210	142	6.59	29820	21.77	0.73	0.11
WPT – 04	240	235	157	6.59	36895	24.35	0.66	0.10
WPT – 05	240	196	162	6.59	31752	11.43	0.36	0.05
WAB – 06	230	205	132	6.59	27060	-	-	-

Where: B = wallette length; H = wallette height; T = wallette thickness; f'_m = masonry compressive strength; A_g = gross area of masonry under prestress; P_{psi} = initial PT force on each bar; and f_{mi} = magnitude of prestress applied to the masonry wallette.

393

394 **Table 3.** Masonry material properties

Measure	f'_b (MPa)	f_r (MPa)	f'_j (MPa)	f'_m (MPa)	C (MPa)	ϕ_s (Ratio)	E_m (GPa)
Mean	17.68	0.40	1.87	6.59	0.43	0.92	1.98
CoV	0.12	0.22	0.15	0.23	-	-	-

Where: CoV = coefficient of variation; f'_b = brick compressive strength; f_r = masonry flexural bond strength; f'_j = mortar compressive strength; f'_m = masonry compressive strength; C = masonry cohesion; ϕ_s = masonry coefficient of friction; and E_m = masonry elastic modulus calculated as $E_m = 300 f'_m$.

395

Table 4. Summary of results

Test Wallette	f_{mi} (MPa)	ε_i (με)	$\varepsilon_{i,t}$ (με)	ε_{tu} (με)	ε_{cu} (με)	k_c (με/MPa)	C_c Ratio	k'_c (με/MPa)	C'_c Ratio	χ -
WPT – 01	1.03	565	521	895	241	234	0.43	278	0.55	0.080
WPT – 02	0.83	476	420	758	193	232	0.40	271	0.54	0.078
WPT – 03	0.73	388	369	637	160	219	0.41	254	0.50	0.073
WPT – 04	0.66	349	334	582	143	217	0.41	247	0.49	0.071
WPT – 05	0.36	222	182	377	65	181	0.29	209	0.41	0.060

Where: f_{mi} = magnitude of prestress applied to the masonry wallette; ε_i = measured masonry elastic shortening; $\varepsilon_{i,t}$ = predicted masonry elastic shortening; ε_{tu} = maximum measured total masonry shortening strain; ε_{cu} = maximum measured masonry creep strain; k_c = measured masonry specific creep; C_c = measured masonry creep ratio; k'_c = extrapolated masonry specific creep; C'_c = extrapolated masonry creep ratio; and χ = aging coefficient empirically determined to match the experimental curve.

397

398   **Table 5.** Prestress loss parameters

Masonry Type	k_{sh} $\mu\varepsilon$	C_c	k_r	
			B	S
URM	0	0.55	0.040	0.025
CM	400	3.00	0.040	0.025

Where: URM = historic unreinforced clay brick masonry; CM = concrete block masonry; B = Grade 500 threaded steel bar; S = seven wire, sheathed and greased strand; C_c = masonry creep parameter; k_c = masonry specific creep; and k_{sh} = masonry shrinkage parameter.

399
400
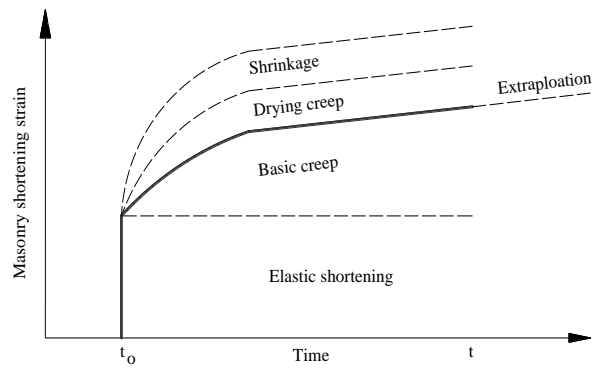
Figures

402

403   **Figure 1.** Time dependent masonry creep

404

(a) Maxwell model   (b) Kelvin model   (c) Burgers model
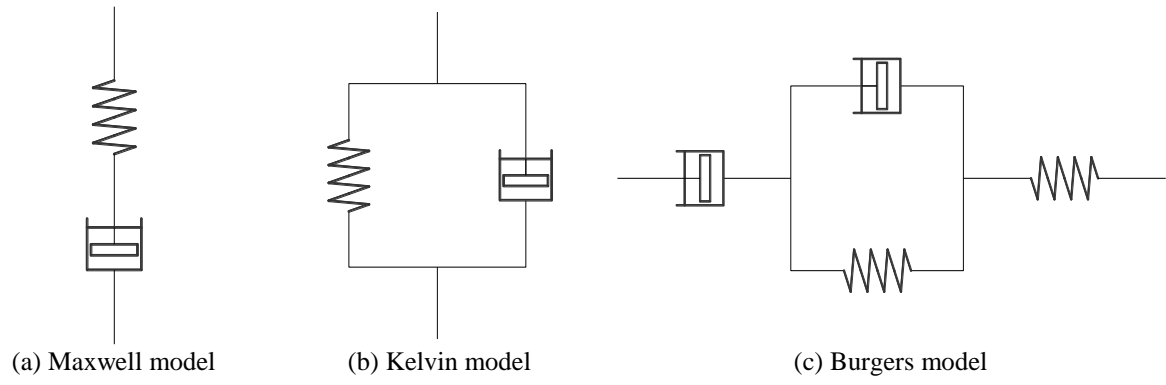
405   **Figure 2.** Representation of basic rheological models
406

(a) After construction in 1881

(b) Being strengthened in 2008

407   **Figure 3.** Old Supreme Court Building

408

(a) cutting of extracted URM section

(b) further cutting to uniform size

Figure 4. Preparation of test wallettes from the extracted URM section

409
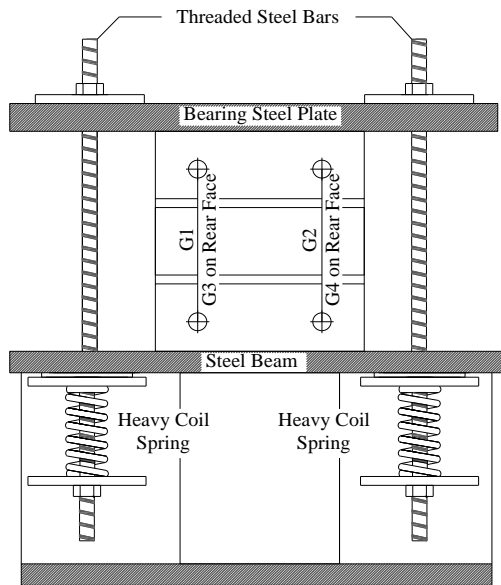
410

411   **Figure 5.** Shrinkage and creep test setup

(a) prestressed wallettes

(b) strain being measured

412 **Figure 6.** Photographs of the masonry shrinkage and creep testing
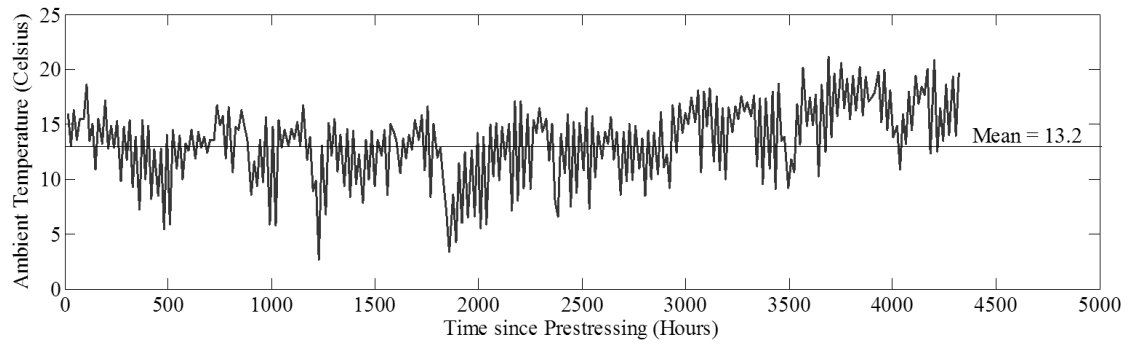
413
414
(a) averaged ambient air temperature
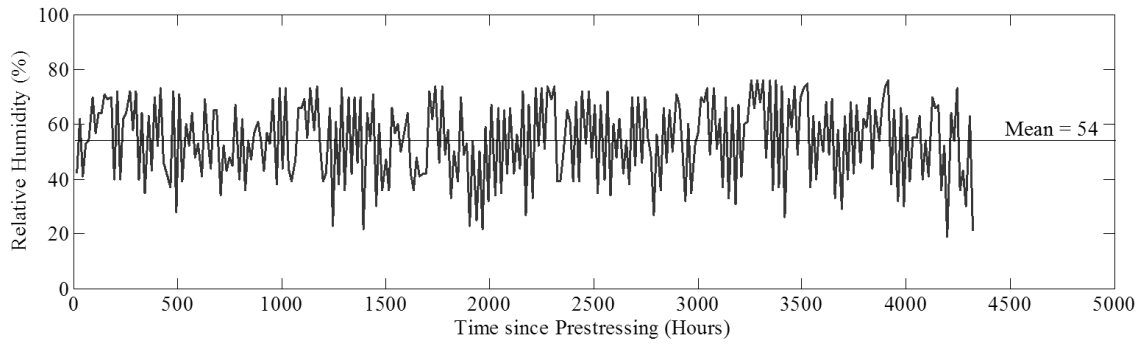
415
416
(b) averaged relative humidity

417   **Figure 7.** Ambient air temperature and relative humidity

418
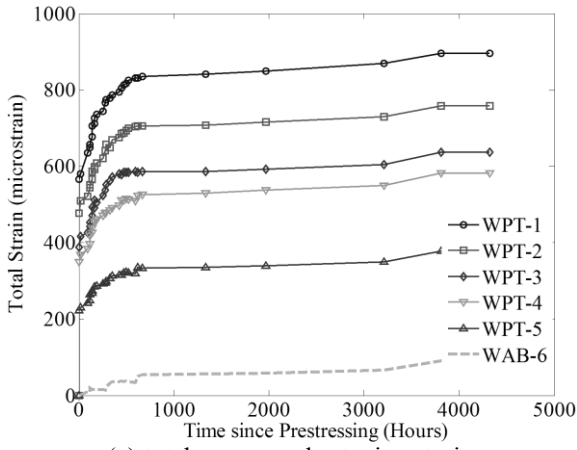
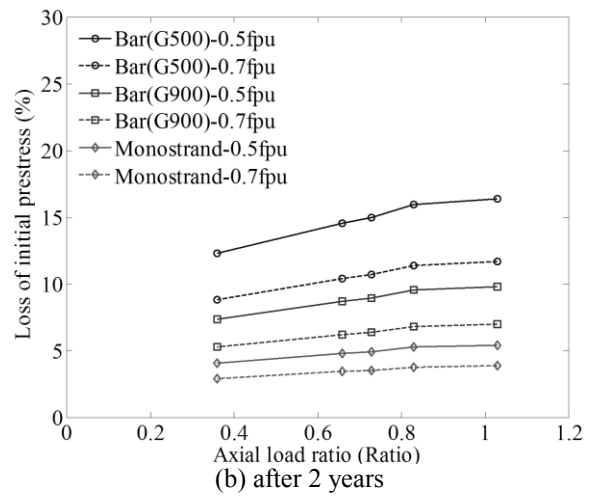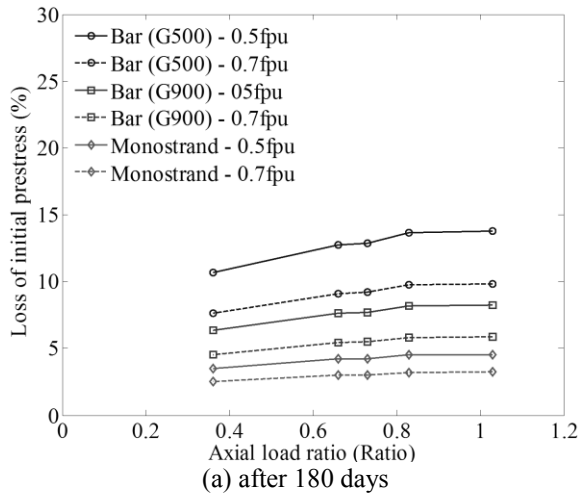(a) total masonry shortening strain
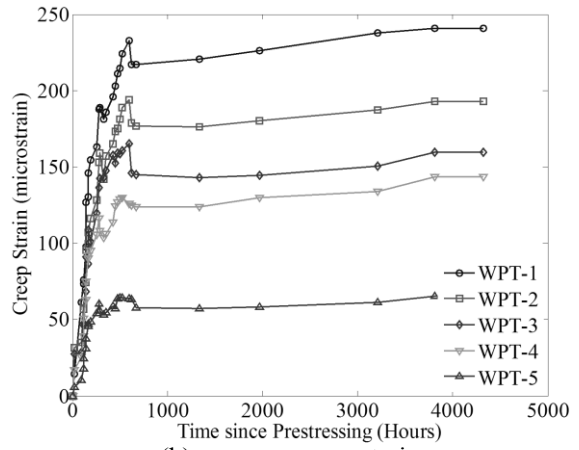
(b) masonry creep strain
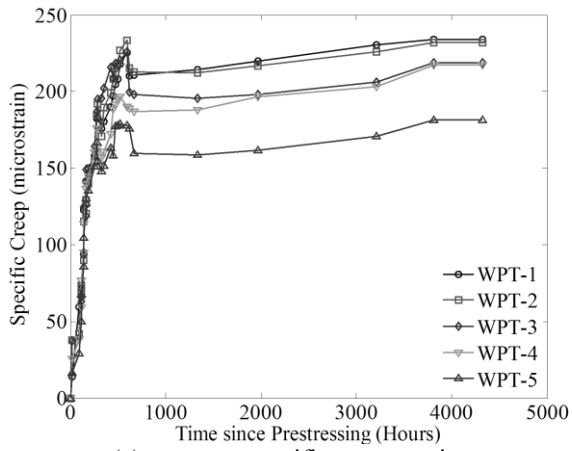
(c) masonry specific creep strain
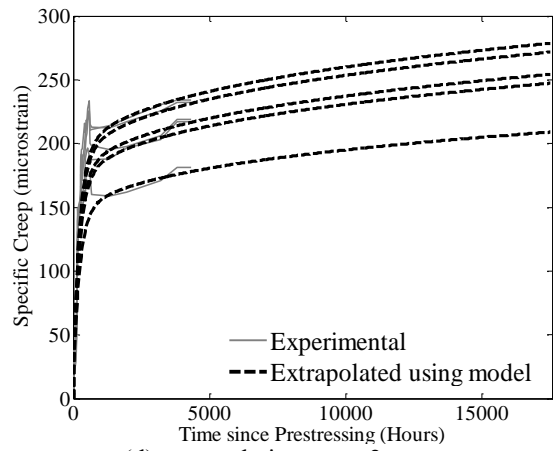
(d) extrapolation up to 2 years

419 **Figure 8.** Time dependent masonry shortening and prestress loss

31

(a) after 180 days   (b) after 2 years

420

Figure 9. Estimated prestress losses